Critical scattering in magnetite*

O. Steinsvoll,† F. Mustoe, L. M. Corliss, and J. M. Hastings
Chemistry Department, Brookhaven National Laboratory, Upton, New York 11973
(Received 6 May 1976)

The energy and wave-vector dependence of the magnetic critical scattering in magnetite has been measured in the vicinity of the 111, 220, and 222 reciprocal-lattice points using a triple-axis neutron spectrometer. The spectral shape function has been found to be Gaussian at the critical point with a characteristic frequency proportional to q^z, where $z = 2.28 \pm 0.05$, 2.30 ± 0.10, and 2.35 ± 0.10, for wave vector $\vec{q}$ measured from 111, 220, and 222, respectively. These values are in reasonable agreement with the dynamic scaling prediction of 2.5. At T_c, the wave-vector-dependent susceptibilities in the vicinity of the three magnetic reflections agree with calculations of de Gennes and Villain. In the spin-wave region, the stiffness constant was found to renormalize with critical index $\sigma' = 0.32 \pm 0.013$, which compares favorably with the value 0.33 predicted by dynamic scaling. Above T_c the inverse range parameter, as determined from three-crystal measurements, showed no site dependence; the critical index ν was found to be 0.79 ± 0.02. Characteristic frequencies of the spectral shape function, measured above T_c, are discussed in relation to the predictions of Résibois and coworkers.

I. INTRODUCTION

As part of a continuing program for studying critical scattering and scaling in prototype materials, we report experimental results on the localized ferrimagnet Fe_3O_4. This material is available as large natural single crystals from iron ores, and all previous investigations of the critical region have been performed on natural specimens. Unfortunately, such crystals have low purity and poor stoichiometry and are generally highly imperfect. Nevertheless, valuable pioneering work on magnetite was performed by Riste and co-workers[1-4] using natural crystals. They determined the sublattice magnetization, the spin-wave dispersion and renormalization, and for the first time observed the magnetic critical scattering near a Bragg reflection. Renormalization of the spin waves in the vicinity of the critical point has also been reported by Jacrot and Cribier.[5] Small-angle critical scattering was observed by Wilkinson and Shull,[6] once again using a natural crystal.

The recent formulation of dynamic scaling theory by Halperin and Hohenberg[7] has renewed interest in the dynamics of magnetic critical phenomena and has prompted a reexamination of magnetite. Whereas most of the work on ferromagnets and antiferromagnets seems to verify the predictions of dynamic scaling,[8-17] a recent investigation by Collins and Saunderson[18] of the magnon renormalization and the energy linewidth in a natural crystal of magnetite near the critical point suggested the possibility of a discrepancy between theory and experiment.

A large synthetic crystal of high quality was recently made available to us by Chikazumi and Todo of the Institute for Solid State Physics, University of Tokyo. It is the same crystal used in a recent study of the Verwey transition by Fujii, Shirane, and Yamada.[19] The present work, using this crystal, repeats and extends the previous work on magnetite in the critical region, with particular emphasis on testing the theoretical predictions of dynamic scaling. In the earlier experiments, critical scattering was measured only around the (111) Bragg reflection, for which the structure factor is a combination of scattering amplitudes of the magnetic ions on A and B sites. In the present work, magnetic critical scattering has been studied around the (111) and also around the (220) and (222), for which the structure factors depend individually on the magnetic ions on A sites and B sites, respectively. In this way one can expect to determine whether or not a site dependence exists in the critical properties. Such a site dependence of the temperature exponent of the magnetization in ferrimagnets has been discussed by van Loef.[20]

Experimental details, together with a discussion of instrumental resolution are presented in Sec. II. The region below T_c is discussed in Sec. III. Here renormalization of the spin-wave stiffness constant is described and compared with the predictions of dynamic scaling theory. Section IV describes the critical scattering at T_c. Analysis of the energy line shape based on various forms of the spectral shape function is discussed and the wave-vector dependence of the characteristic frequency is compared with the dynamic scaling predictions. Quasielastic scattering above T_c is treated in Sec. V, where measurements of the temperature dependence of the range parameter are presented. The spectral shape function

is further discussed and linewidths are compared with explicit calculations of Résibois and Piette.[21] Some general conclusions are presented in Sec. VI.

II. EXPERIMENTAL

The crystal was in the shape of a cylinder 10 mm in diameter, 15 mm in height with the [111] axis parallel to the cylinder axis. To prevent any changes in stoichiometry during the heating, the crystal was enclosed in an evacuated quartz jacket which, however, allowed for thermal expansion. The vacuum furnace consisted of hollow copper spherical caps, with heater wires on the outside, joined to a cylindrical equatorial section which was thinned out to allow for the passage of neutrons. Two cylindrical thermal shields were inserted between the heating unit and the outer aluminum vacuum jacket. The temperature was regulated by means of a three-parameter electronic controller which maintained stability to one part in 10 000. The sample crystal was mounted in the center of the copper sphere with a thermocouple adjacent to it to provide a relative measure of the temperature. The cylinder axis [111] was horizontal and the [110] axis vertical. With this orientation, all interesting reflections could be reached.

The triple-axis spectrometer was operated in the constant-$\vec{Q}$ mode for all experimental runs. Single crystals of germanium were used as monochromator and analyzer. The monochromatic neutron beam had an energy $E_i = 14$ meV ($\lambda = 2.417$ Å) and was obtained by Bragg reflection from (111). A pyrolytic graphite filter was used to further reduce the $\frac{1}{2}\lambda$ contamination. Soller slits having individual horizontal divergences of 20′ were inserted before and after both the monochromator and analyzer. As no vertical collimator was used, the vertical divergence was limited by the size of beam openings, sample size, and distances between components of the system.

The parameters of the instrumental resolution function (mosaic spreads and effective collimator apertures) were determined by experiment.[22] The mosaic spread parameters of the Ge crystals, as determined from rocking curves, were $6.5' \pm 0.5'$ (half width at half-maximum). The horizontal collimation parameter was obtained from a sharp Bragg reflection by rocking the collimator with crystal fixed. The collimation parameter α used in the resolution function is the standard deviation of the Gaussian approximation to the triangular transmission function of the slit and is proportional to the geometrical slit aperature α', with a proportionality constant of 0.425 for an ideal system. The experimental constant, giving the best fit to the rocking curve, was found to be 0.446. The effective vertical component of the resolution function was determined by fitting a Gaussian to the rocking curve obtained by rotating the sample about a horizontal axis perpendicular to the scattering vector.

III. MAGNON RENORMALIZATION BELOW T_c

Spin-wave theory predicts a quadratic dispersion law

$$E = Dq^2 \tag{1}$$

for the low-energy excitations in a ferrimagnet at temperatures below the critical point.[23] One also expects a diffusive mode connected with the longitudinal component of magnetization. In our experiments we found only the spin-wave bands connected with creation and annihilation of spin waves. (A small peak centered at $E = 0$ was in fact observed, but its intensity did not change in going from room temperature to T_c and it was attributed to elastic background scattering.) According to dynamic scaling theory,[7] the spin-wave stiffness constant D should renormalize to zero at T_c according to the law

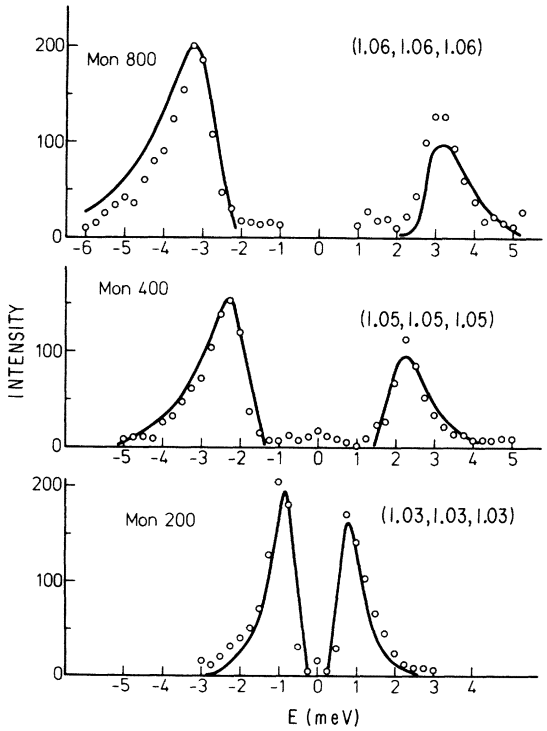

FIG. 1. Experimental spin-wave peaks for a series of constant-$\vec{Q}$ scans at $T = T_c - 200$ °K. The curves are the result of simulating the experiments by means of a computer program, as explained in the text. Curves are labeled with reciprocal-lattice coordinates and monitor scale factors.

$$D = C[(T_c - T)/T_c]^{\sigma'}, \quad (2)$$

where the exponent $\sigma' \approx 0.33$.

We have performed constant-$\vec{Q}$ scans at a series of different temperatures below the transition temperature T_c. Typical triple-axis scans are shown in Fig. 1 for $T_c - 200$ K. The peaks are due to creation ($\Delta E > 0$) and annihilation ($\Delta E < 0$) of magnons in the crystal. The strongest magnon signals are expected around the (111) reflection since this reflection is mainly of magnetic origin and the form factor is large. The experiments below T_c were therefore confined mainly to this reflection. The magnon peaks were obtained for radial directions of $\vec{Q}$ in reciprocal space. This was done in order to keep the same orientation as in the experiments on the diffusive mode at T_c and above, so that low-temperature background data would be available for corrections to the critical scattering. This means, however, that the magnons were not well focused.

We see from Fig. 1 that the kinematic factor k'/k dominates over the Boltzmann factor because the intensity is higher for annihilation than for creation. We also observe from Fig. 1 that the magnon peaks are not symmetric around the positions of the maxima. This is due to the interplay between the resolution function of the spectrometer and the magnon dispersion surface of the sample. Because of the quadratic nature of the dispersion law, the resolution ellipsoid of the instrument has a stronger interaction with the dispersion surface for energy settings on the "inside" of the paraboloidal cup. This gives rise to the tails at higher-energy transfers, both for creation and annihilation. One could well imagine, therefore, that the energy value corresponding to the peak intensity might not represent the magnon dispersion curve at the chosen momentum transfer.[24] In order to study the extent of such displacements, if any, the spectrometer scans were simulated on a computer by convoluting the resolution function of our spectrometer with a sharp excitation function, i.e., ignoring lifetime effects. The results of such calculations have also been indicated in Fig. 1, where it is seen that with a proper choice of D, both the shape and relative intensities of experimental peaks could be reproduced with good accuracy. No measurable shift in the peak position could be detected, however. It was therefore concluded that the corresponding values of energy and momentum could be read off directly from the experimental curves without correction. In Table I we list the results obtained at $T_c - 25$ K as an example.

Assuming a quadratic dispersion law, as a first approximation, a spin-wave stiffness constant

TABLE I. Experimental magnon energies at $T = T_c - 25$ K.

Reciprocal-lattice point	q (Å^{-1})	$\Delta E < 0$ (meV)	$\Delta E > 0$ (meV)
(2.02, 2.02, 0)	0.0210	0.15	0.15
(1.02, 1.02, 1.02)	0.0259	0.20	0.20
(2.03, 2.03, 0)	0.0315	0.30	0.30
(1.03, 1.03, 1.03)	0.0386	0.55	0.50
(2.04, 2.04, 0)	0.0420	0.60	0.60
(1.04, 1.04, 1.04)	0.0515	0.90	0.90
(2.06, 2.06, 0)	0.0630	1.5	1.35
(1.94, 1.94, 0)	0.0630	1.25	1.25
(1.06, 1.06, 1.06)	0.0772	1.75	1.75
(0.94, 0.94, 0.94)	0.0772	1.75	1.55
(2.06, 2.06, 2.06)	0.0772	1.75	1.80
(1.94, 1.94, 1.94)	0.0772	1.75	1.75
(2.08, 2.08, 2.08)	0.1029	3.0	3.0

D was fitted to the q dependence of the magnon energy by a nonlinear least-squares program.[25] The resulting values of D for various temperatures are listed in Table II. A dispersion law containing a fourth-order term was also tested. The resulting values of D were somewhat larger and the extra term had negative sign. The uncertainties were, however, also larger, indicating that no improvement in the fit was obtained by including a fourth-order term. Equation (2) for the temperature dependence of D was then fitted to the experimental data by the nonlinear least-squares program in which the normalized temperatures and the corresponding values of D were assumed to be known. The least-squares standard deviations in D were used for calculating the relative weights, $w = 1/(\Delta D)^2$. The results of the fitting were

$$\sigma' = 0.32 \pm 0.013, \quad C = 850 \pm 25.$$

This is in good agreement with the theoretically expected exponent noted above. The experimental points and the least-squares fit are shown in Fig. 2. In similar experiments on a natural crys-

TABLE II. Temperature dependence of the spin-wave stiffness constant.

$T_c - T$ (K)	$(T_c - T)/T_c$	D (meV Å^2)	ΔD
3.25	3.8×10^{-3}	126	6
5	5.8×10^{-3}	166	4
9	0.01	232	20
15	0.0175	244	10
25	0.029	298	6
50	0.058	335	5
100	0.117	437	5
200	0.234	521	6

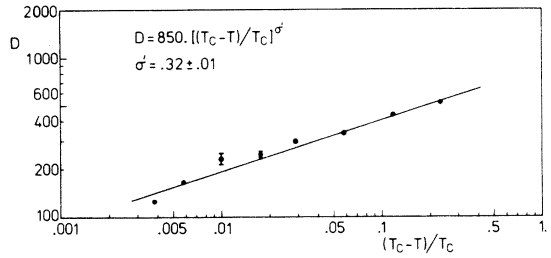

FIG. 2. Renormalization of the spin-wave stiffness constant D.

tal of magnetite, Collins and Saunderson[18] found the exponent to be 0.26 ± 0.03.

The above analysis requires, of course, a knowledge of T_c on the arbitrary temperature scale of the experiment. It was determined in the following manner. With the spectrometer set for zero energy transfer and a small arbitrary value of $\vec{q}$, the intensity of the critical scattering was measured as a function of temperature and the temperature corresponding to maximum intensity, T_{max}, was noted. This procedure was repeated for decreasing values of $\vec{q}$ and the values of T_{max} extrapolated to $\vec{q}=0$ to give T_c. On the temperature scale of the experiment, this was 855.0 ± 0.1 K.

IV. CRITICAL SCATTERING AT T_c

The general expression for the cross section for magnetic critical scattering in the vicinity of T_c, after correcting for the magnetic form factor and for energy-dependent and thermal factors, can be written

$$\frac{d^2\sigma}{d\omega d\Omega} \propto \chi(\vec{q}) F(\vec{q}, \omega), \tag{3}$$

where $\chi(\vec{q})$ is the wave-vector-dependent susceptibility and $F(\vec{q}, \omega)$ is the spectral shape function. The analytical form of $F(\vec{q}, \omega)$ is generally unknown. One may, however, define a characteristic frequency $\Gamma_\kappa(\vec{q})$ such that

$$\int_{-\Gamma_\kappa(\vec{q})}^{+\Gamma_\kappa(\vec{q})} F(\vec{q}, \omega)\, d\omega = \frac{1}{2}, \tag{4}$$

where κ is the inverse range parameter.

Dynamic scaling theory[7] predicts that at T_c the characteristic frequency has the following form:

$$\Gamma_\kappa(\vec{q}) = \Gamma_0(\vec{q}) = \alpha q^z, \tag{5}$$

where α is a constant. For an isotropic ferromagnet, the theoretical value of the exponent z is $\frac{5}{2}$, whereas for an antiferromagnet it is $\frac{3}{2}$. This difference is connected with the fact that in ferromagnets the total moment is a conserved quantity. In a ferrimagnet like magnetite, the total moment is also conserved and it is expected therefore that the value of z should be the same as in the ferromagnetic case.[26]

In order to analyze the data one must have analytical forms of $\chi(\vec{q})$ and $F(\vec{q}, \omega)$. In view of the limited precision of the three-crystal data, $\chi(\vec{q})$ was taken to have the simple Ornstein-Zernike form:

$$\chi(\vec{q}) = Y_1/(\kappa^2 + q^2), \tag{6}$$

where Y_1 combines an interaction constant and a normalizing factor. de Gennes and Villain[27] have shown that for the case where the unit cell contains more than one kind of magnetic ion and a multiplicity of lattice sites, the quantity Y_1 should depend on the reciprocal-lattice point about which $\chi(\vec{q})$ is measured. For the particular case of magnetite they have calculated the value of Y_1 to be expected in the vicinity of T_c for critical scattering close to the (111), (220), and (222) Bragg positions. In this calculation they have used Néel's values for the exchange constants J_{AA} and J_{AB} and a consistent value of T_c.

In the absence of any theoretical basis for the choice of the mathematical form of $F(\vec{q}, \omega)$, we have tested both Gaussian (G) and Lorentzian (L) approximations. These functions, in combination with $\chi(\vec{q})$ were convoluted with the resolution function, and the width Γ as well as the constant Y_1 were adjusted by least squares for the best fit to the experimental data. From inspection of the least-squares residues, it was clear that the experimental data were much better approximated by a G-model cross section. Not only were the residues consistently lower for the G model, but the variation of Y_1 with change in $\vec{q}$ was much smaller for the G model. (As we will see later, in the discussion of results, a small variation of Y_1 with $\vec{q}$ is to be expected.) Another check on the appropriateness of the G model was provided by an additional criterion of internal consistency which will be discussed at the end of this section.

With this justification, a Gaussian function was used for the initial analysis of the experimental data obtained around the (111), (220), and (222) reflections. [A more refined analysis of the (111) data will be presented later.] It is worth noting, however, that the choice between G and L models depends critically on a knowledge of the background in the energy scan. Drawing the base line too low over the limited range of the ω scan will produce wings that are typical of an L function. Furthermore, at temperatures below T_c, one observes a small elastic peak ($\omega = 0$) which must be subtracted as an extra background effect. Underestimating this elastic background will also favor a least-squares fit to an L function. The backgrounds in the present experiments were first determined by going to large values of $|\omega|$ for temperatures at

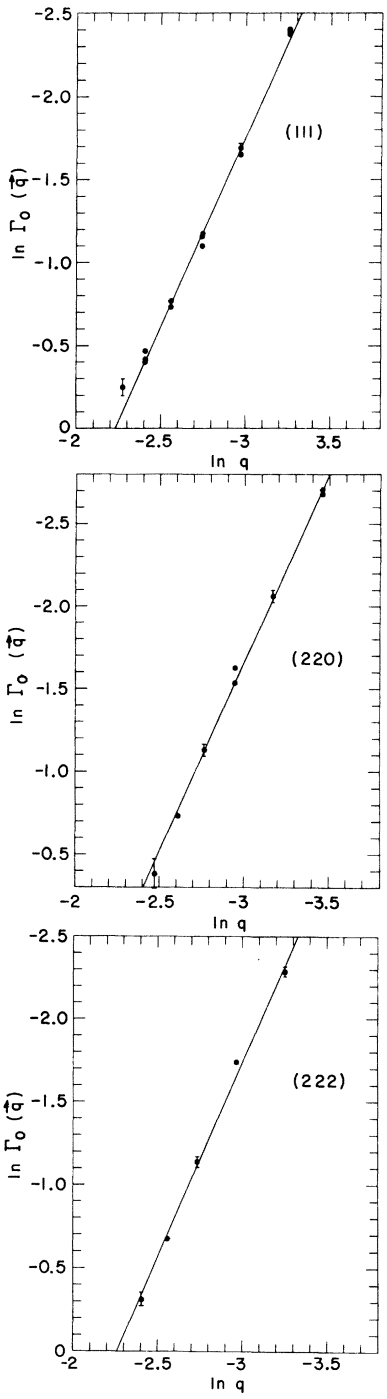

FIG. 3. Characteristic frequency at T_c as a function of q for various magnetic reflections.

and above T_c. A second measurement was made at temperatures much below T_c where the background was essentially constant in the regions away from the elastic position and the magnon bands. The two measurements of the background were approximately the same and the final value used to correct our data was obtained by averaging these two results.

TABLE III. Exponent z in the expression $\Gamma_0(q) = \alpha q^z$.

hkl	z	q range[a] (Å^{-1})
111	2.28 ± 0.05	0.0386 – 0.0901
220	2.30 ± 0.10	0.0315 – 0.0840
222	2.35 ± 0.10	0.0386 – 0.0901

[a] $\vec{q}$ points along the scattering vector.

Thus the analytical form of the cross section in Eq. (3), at T_c, was taken to be

$$\frac{d^2\sigma}{d\omega d\Omega} = (Y_1/q^2)\exp(-\omega^2/\text{const}\,\Gamma^2)\,. \tag{7}$$

To take account of the small variation of Γ over the resolution volume, the expression

$$\Gamma = Y_2 q^{2.5} \tag{8}$$

was inserted in the cross section. If the dynamic scaling prediction[7] of 2.5 for the exponent z in Eq. (5) is exact, then Y_2 should be a constant. On the other hand, if the exponent is incorrect, Y_2 would be expected to exhibit a $\vec{q}$ dependence to compensate for this error.

At each value of $\vec{q}$, a least-squares fit of the convoluted cross section was made to the data, and the best values of the parameters Y_1 and Y_2 were obtained. For a given reciprocal-lattice point, the value of Y_1 should, in principle, have been constant, whereas in reality it showed a slight trend with $\vec{q}$. This is largely a geometrical effect produced by the rotation of the sample in the beam about an axis normal to $2\pi\vec{\tau}$. The values of Y_2 obtained from the fits were not quite constant either; a very slow variation with q was found, indicating a small departure of the exponent z from the value 2.5, assumed for the purposes of the resolution correction. The value of Y_2 giving the best fits to the data were converted to characteristic frequencies using (8). A model function of the form $\Gamma = Cq^z$ was then fitted to these characteristic frequencies by least squares and the best value of z obtained. This new value of z was inserted in the expression for the cross section and the procedure was repeated until self-consistent values of z were obtained.

Figure 3 shows log-log plots of the data obtained around the three different reciprocal-lattice points, together with curves representing the best fits. Table III gives the values of the exponents together with the range of q over which the data were collected. The quoted errors are twice the standard deviations given by the least-squares analysis. These values of z agree reasonably well with the

dynamic scaling prediction of 2.5. The fact that all three z values are essentially equal eliminates the possibility of any significant site dependence of the critical fluctuations.

We may now compare the best value of Y_1 obtained for each series of experiments with the theoretical calculations of de Gennes and Villain.[27] To eliminate the experimental instrument factor, we have divided the average experimental values of Y_1 corresponding to a given (hkl) by the theoretical value and have examined the constancy of this ratio for the various reflections. From Table IV we see that the agreement is satisfactory. The small variation from one reflection to another may have an experimental as well as a theoretical origin.

Returning to the question of the mathematical form of the function used to represent $F(\vec{q}, \omega)$, we note that the iterative procedure described above for determining the exponent z converged very rapidly in the case of the Gaussian model. This was not true in the case of the Lorentzian, where successive iterations forced the value of z to unacceptably high values.

In order to see whether some functional form intermediate between a Gaussian and a Lorentzian might give a still better fit to the data, the spectral shape function was taken to be a linear combination of a Gaussian and a Lorentzian having equal widths[28]:

$$F = \alpha \frac{(\Gamma/2)^2}{(\Gamma/2)^2 + \omega^2} + (1-\alpha)\exp(-\omega^2/b^2\Gamma^2), \qquad (9)$$

where Γ is the full width at half maximum and $b = 0.600561$. This expression was combined with $\chi(\vec{q})$ and convoluted with the resolution function for comparison with experimental intensities near the 111 reciprocal-lattice point, where the accuracy was greatest. The best values of α, as well as the corresponding values of Y_1 and Y_2, were then obtained by least squares. The smallest residues were obtained for $\alpha = 0$, confirming once again the earlier indication of the superiority of the Gaussian model.

TABLE IV. Comparison of observed and calculated relative values of Y_1 at T_c.

hkl	Expt. (arb. scale)	Theor.	10^5 ratio
111	0.0208	1230	1.69
220	0.009 09	550	1.65
222	0.0247	1375	1.80

V. CRITICAL SCATTERING ABOVE T_c

The quasielastic scattering around the 111, 220, and 222 reciprocal-lattice points was also investigated above T_c, for a series of q values. The temperature difference $T - T_c$ was varied in steps from 2 to 25 K. In this temperature range κ takes on finite values and there are now three parameters, Y_1, Y_2, and κ which should, in principle, be varied in the least-squares fit. However, because of the high correlation between Y_1 and κ only one of the two is adjustable.

The Gaussian and Lorentzian contributions to the peak shape at temperatures above T_c were studied by means of a procedure similar to that described at the end of the preceding section. Due to convergence difficulties of the program, it was found necessary to fix the value of κ rather than that of Y_1. The approximate κ values used for this test were obtained by integrating the intensities of the quasielastic peaks, correcting for the background, and plotting the inverse of the integrated peak as a function of q^2. The points lay on a line whose intercept with the abscissa give a value of κ for each temperature. There are certain errors inherent in this approach since it ignores q-dependent resolution effects produced by the tipping of the resolution ellipsoid away from the ω axis. Nevertheless, because of the strong correlation between κ and Y_1, an error in κ is compensated by a corresponding shift in Y_1 in the least-squares fit, *without* appreciably affecting the shape analysis. This study was carried out only for the 111 data, inasmuch as the lower precision of the less intense 220 and 222 data did not warrant a more refined treatment. The analysis showed that all peaks were close to being Gaussian ($\alpha \sim 0.2$), but the nonzero value of α suggests that there is an extra contribution in the wings, i.e., a small tendency toward Lorentzian character.

In view of the small size of the deviation from Gaussian shape, the temperature dependence of κ was studied by fitting the data with a pure Gaussian spectral shape function together with an Ornstein-Zernike susceptibility. With the restriction to the Gaussian shape function there were no convergence problems and the fits were performed with Y_1 fixed at the value obtained at T_c. It is to be noted that κ is determined by the best fit to both the q and ω dependence of the scattering around a given reciprocal-lattice point. Although statistics are poorer than in the conventional two-crystal method, the procedure is free of errors associated with the quasielastic approximation. (Ideally, of course, both kinds of measurements should be combined to give the best determination of κ.) At each temperature the observed values

of κ showed good internal consistency for different reflections and there were no systematic trends. In Table V we show the average values of κ obtained at various temperatures and reciprocal lattice points. A model function of the form $\kappa = A(\Delta T)^{\nu}$ was fitted by least squares to this data giving

$$\nu = 0.79 \pm 0.02, \quad A = 1.25 \pm 0.13.$$

The log-log plot of Fig. 4 shows the fit to the experiment points. The value obtained for ν depends somewhat on the choice of function used to represent the wave-vector-dependent susceptibility. For example, use of the Fisher approximant[29] would have resulted in about a 2% decrease in ν if the critical exponent η were as large as 0.05.

For the isotropic Heisenberg ferromagnet, Ritchie and Fisher[30] have calculated that $\nu = 0.70$ for all lattices and all spins. Our experimental value for ν appears to be significantly higher than this. If electron hopping between Fe^{2+} and Fe^{3+} ions on the B sites is sufficiently slow, then we may expect a theoretical description in terms of a random site-dilution problem to be appropriate. Current theory concerning the expected behavior of the critical exponents is divided.[31] High-temperature series studies[32,33] predict, with considerable uncertainty, that the critical exponent γ (and also ν) should increase with increasing randomness, in agreement with our experimental result. The renormalization group approach,[34] on the other hand, predicts no change on randomization. At the present time we cannot say that our experimental accuracy is clearly sufficient to favor one type of theory over the other.

We now consider the behavior of the energy width of the critical scattering in the region above T_c. According to dynamic scaling theory, the characteristic frequency $\Gamma_\kappa(\vec{q})$ is a homogeneous function of $\vec{q}$ and κ, and we may write for $T > T_c$

$$\Gamma_\kappa(\vec{q}) = \Gamma_0(\vec{q}) f(\kappa/q), \tag{10}$$

where $\Gamma_0(\vec{q})$ is given by Eq. (5). The function f has been calculated by Résibois and Piette,[21] using the theory of Résibois and De Leener.[35] The form of the function is such that for a given

TABLE V. Weighted mean value of κ.

$T - T_c$	(111)	(220)	(222)
2	0.0107 ± 0.0006	0.0114 ± 0.0001	
3.5	0.0158 ± 0.0014	0.0141 ± 0.0010	
8.75	0.0365 ± 0.0023	0.0345 ± 0.0037	0.0350 ± 0.002
15	0.0533 ± 0.0030	0.0481 ± 0.0020	0.0514 ± 0.002
25	0.0775 ± 0.0028		

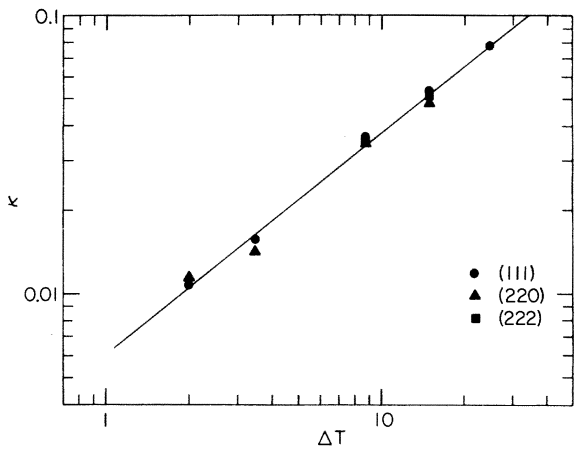

FIG. 4. Temperature dependence of the inverse range parameter κ showing best fit obtained by least squares.

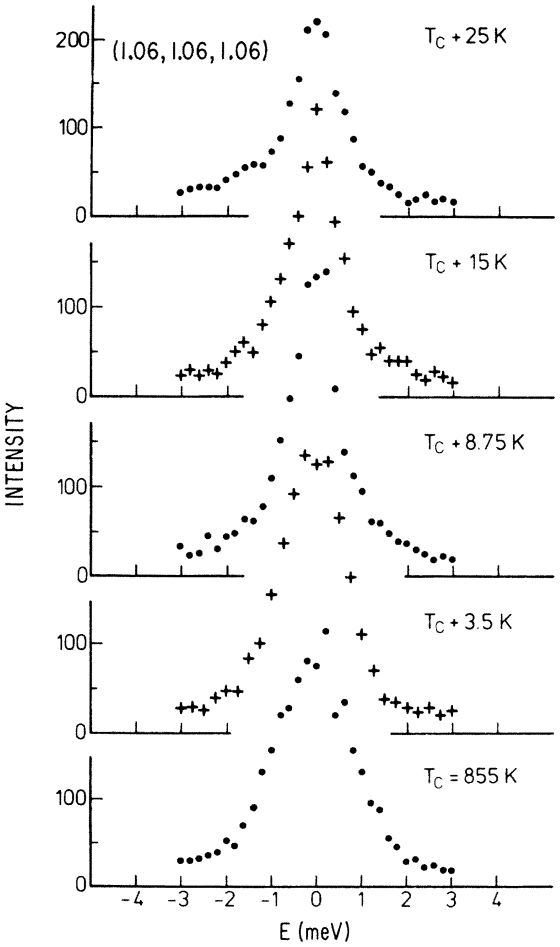

FIG. 5. Constant-$\vec{Q}$ energy scans at the reciprocal-lattice point (1.06, 1.06, 1.06) for various temperatures above T_c.

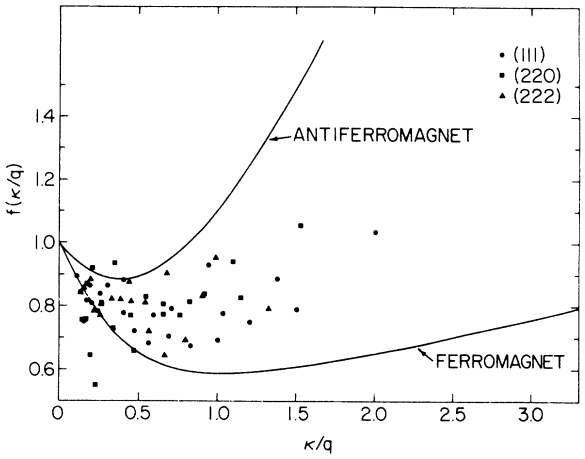

FIG. 6. Dependence of normalized characteristic frequencies on κ/q. The curves represent the theoretical function $f(\kappa/q)$ of Résibois and co-workers (Refs. 21 and 35) for ferromagnets and antiferromagnets.

value of q one should observe a progressive narrowing of the quasielastic reflection as κ increases with temperature for $\kappa < q$ and an increasing width for $\kappa > q$. This effect can be seen in the typical experimental curves of Fig. 5.

Characteristic frequencies of the quasielastic peaks were obtained from the least-squares fit of the Gaussian model cross section. These characteristic frequencies were divided by the corresponding values at the critical temperature and the ratios have been plotted as a function of κ/q in Fig. 6. The curves shown in the figure represent the theoretical functions $f(\kappa/q)$ for ferromagnets and antiferromagnets. It is seen that the experimental values show the expected trend but fall between the two theoretical curves. We have no explanation of the failure of the experimental points to follow more closely the ferromagnetic curve. One possibility is that the inherent shape of the critical scattering changes with temperature, in which case the normalization procedure for obtaining experimental values of $f(\kappa/q)$ would be incorrect.

VI. CONCLUSION

Our experiments have shown that the behavior of ferrimagnetic Fe_3O_4 at the critical point and in its vicinity is in general agreement with the theoretical predictions of dynamic scaling theory for ferromagnets. In the crystal, the magnetic ions on A and B sites are coupled antiferromagnetically, but the moments on the two kinds of sites are uncompensated, thus giving rise to macroscopic magnetization. Our results confirm the expectation that, as long as the total moment is a conserved quantity, magnetite should exhibit critical behavior typical of a ferromagnet. Furthermore, the data indicate the absence of any site dependence in the critical properties measured.

ACKNOWLEDGMENTS

We are indebted to D. Huber, P. Hohenberg, and S. Lovesey for illuminating discussions.

*Work performed under the auspices of the U. S. Energy Research and Development Administration.

†Permanent address: Institutt for Atomenergi, 2007 Kjeller, Norway.

[1]A. W. McReynolds and T. Riste, Phys. Rev. 95, 1161 (1954).

[2]T. Riste, K. Blinowski, and J. Janik, J. Phys. Chem. Solids 9, 153 (1959).

[3]T. Riste, J. Phys. Chem. Solids 17, 308 (1961).

[4]T. Riste and L. Tenzer, J. Phys. Chem. Solids 19, 117 (1961).

[5]B. Jacrot and D. Cribier, J. Phys. Radium 23, 494 (1962).

[6]M. K. Wilkinson and C. G. Shull, Phys. Rev. 103, 516 (1956).

[7]B. I. Halperin and P. C. Hohenberg, Phys. Rev. 177, 952 (1969).

[8]M. F. Collins, V. J. Minkiewicz, R. Nathans, L. Passell, and G. Shirane, Phys. Rev. 179, 417 (1969).

[9]V. J. Minkiewicz, M. F. Collins, R. Nathans, and G. Shirane, Phys. Rev. 182, 624 (1969).

[10]H. Y. Lau, L. M. Corliss, A. Delapalme, J. M. Hastings, R. Nathans, and A. Tucciarone, Phys. Rev. Lett. 23, 1225 (1969).

[11]J. Als-Nielsen, Phys. Rev. Lett. 25, 730 (1970).

[12]M. P. Schulhof, P. Heller, R. Nathans, and A. Linz, Phys. Rev. B 1, 2304 (1970).

[13]The Neutron Inelastic Scattering Group and M. Tournarie, Phys. Lett. A 31, 561 (1970).

[14]R. Kahn and G. Parette, J. Phys. (Paris) 32, C1-523 (1970).

[15]V. J. Minkiewicz, in *Dynamical Aspects of Critical Phenomena*, edited by J. I. Budnick and M. P. Kawatra (Gordon and Breach, New York, 1972), p. 69.

[16]A. Tucciarone, J. M. Hastings, and L. M. Corliss, Phys. Rev. B 8, 1103 (1973).

[17]O. W. Dietrich, J. Als-Nielsen, and L. Passell (unpublished).

[18]M. F. Collins and D. H. Saunderson, J. Appl. Phys. 41, 1433 (1971).

[19]Y. Fujii, G. Shirane, and Y. Yamada, Phys. Rev. B 11, 2036 (1975).

[20]J. J. van Loef, Solid State Commun. 4, 625 (1966).

[21]P. Résibois and C. Piette, Phys. Rev. Lett. 24, 514 (1970). See also C. Joukoff-Piette and P. Résibois, Phys. Lett. A 42, 531 (1973) for tables of numerical

values for both the ferromagnet and the antiferromagnet.

[22]A. Tucciarone, H. Y. Lau, L. M. Corliss, A. Delapalme, and J. M. Hastings, Phys. Rev. B 4, 3206 (1971).

[23]For a summary of theoretical and experimental work on Fe_3O_4, see H. A. Alperin, O. Steinsvoll, R. Nathans, and G. Shirane, Phys. Rev. 154, 508 (1967).

[24]E. J. Samuelsen, in *Structural Phase Transitions and Soft Modes* (Universitetsforlaget, Oslo, 1971).

[25]D. R. Powell and J. R. Macdonald, Comput. J. 15, 148 (1972).

[26]P. C. Hohenberg and J. B. Swift, J. Phys. C 7, 4009 (1974).

[27]P. G. de Gennes and J. Villain, J. Phys. Chem. Solids 13, 10 (1960). The attention of the reader is called to the existence of a number of typographical errors in the formulas on p. 24 of this reference. The computed values for $g(hkl)$ on p. 25, which are of interest here, are correct, however.

[28]G. K. Wertheim, M. A. Butler, K. W. West, and D. N. E. Buchanan, Rev. Sci. Instrum. 45, 1369 (1974). The function in Eq. (9) was used by these authors to represent (without convolution) experimental Voigt profiles which are themselves convolutions of Lorentzians with Gaussians.

[29]M. E. Fisher, J. Math. Phys. 5, 944 (1964).

[30]D. S. Ritchie and M. E. Fisher, Phys. Rev. B 5, 2668 (1972).

[31]G. A. Baker, Jr., J. C. Bonner, and M. Blume (private communication).

[32]D. C. Rapaport, J. Phys. C 5, 1830 (1972).

[33]G. S. Rushbrooke, R. A. Muse, R. L. Stephenson, and K. Pirnie, J. Phys. C 5, 3371 (1972).

[34]A. Aharony, Y. Imry, and S-K. Ma, Phys. Rev. B 13, 466 (1976).

[35]P. Résibois and M. De Leener, Phys. Rev. 178, 806 (1964).